

Aerodynamics and Flight Capability of a Supersonic Flight Experiment Vehicle

By Kazuhide MIZOBATA,¹⁾ Yoshihiro SUZUKI,¹⁾ Sakae OOISHI,¹⁾ Satoshi KONDOH,¹⁾ Takakage ARAI²⁾
and Kazuyuki HIGASHINO¹⁾

¹⁾Aerospace Plane Research Center (APReC), Muroran Institute of Technology, Muroran, Japan

²⁾Dept. of Aerospace Engineering, Osaka Prefecture University, Sakai, Japan

(Received July 31st, 2015)

With the aims of creating and validating innovative fundamental technologies for high-speed atmospheric flights, a small scale supersonic flight experiment vehicle is designed as a flying test bed. An aerodynamic configuration is proposed for the 2nd-generation vehicle with a cranked-arrow main wing and a single Air Turbo Ramjet Gas-generator-cycle (ATR-GG) engine. Its longitudinal, lateral, and control surface aerodynamics are characterized through intensive wind-tunnel tests. They are found to be quite moderate except that the directional stability deteriorates severely at large angles of attack and side slip, and that the elevon deflections for roll control cause adverse yaw. These aerodynamic anomalies will result in a tendency of roll reversal at large angles of attack. It can be prevented to some extent by coordinated rudder deflections. In addition, necessity of transonic drag reduction is clarified through thrust margin and flight capability analyses. Probability of 5 to 20 % drag reduction in the transonic regime (Mach 0.8 to 1.2) is demonstrated by configuration modification on the basis of the area rule at Mach 1.1.

Key Words: Space Transportation, Flying Test Bed, Flight Test, Supersonic, Jet Propulsion

Nomenclature and Abbreviations

AADP	: aileron alone departure parameter
AOA	: angle of attack
C_D	: drag coefficient
$C_{D,0}$: zero-lift drag coefficient
C_L	: lift coefficient
C_l	: rolling moment coefficient
C_m	: pitching moment coefficient
C_n	: yawing moment coefficient
CG	: center of gravity
I	: moment-of-inertia matrix
k	: rudder gain
k_e	: elevon gain
L	: rolling moment
LCDP	: lateral control departure parameter
M	: flight or flow Mach number or pitching moment
MAC	: mean aerodynamic chord
\vec{M}_b	: aerodynamic moments vector with respect to the body-fixed coordinates
N	: yawing moment
α	: angle of attack
β	: side slip angle
δ_a	: deflection angle of aileron
δ_e	: deflection angle of elevon
δ_r	: deflection angle of rudder
ψ	: yaw angle
$\vec{\Omega}_b$: angular velocity vector with respect to the body-fixed coordinates

1. Introduction

Innovation in technologies for high-speed atmospheric flights is essential for establishment of supersonic/hypersonic and reusable space transportations. It is quite effective to verify such technologies through small-scale flight tests repeatedly in practical high-speed environments prior to installation to large-scale vehicles. Thus we are developing a small-scale supersonic flight experiment vehicle as a flying test bed.

We have proposed two generations of aerodynamic configuration with a cranked-arrow main wing. In the 1st generation, twin counter-rotating axial fan turbojet (CRAFT) engines¹⁾ were proposed for propulsion. The aerodynamics and flight capability of the configuration were analyzed through wind-tunnel tests and three-degree-of-freedom flight trajectory calculations. In addition, a full-scale prototype vehicle was designed and fabricated in order to verify the subsonic flying characteristics of the 1st-generation configuration through flight tests. Its appropriate flying characteristics were demonstrated through subsonic flight tests in August 2010.²⁾

On the other hand, a revised aerodynamic configuration has been proposed for the 2nd-generation vehicle with a single Air Turbo Ramjet Gas-generator-cycle (ATR-GG) engine.³⁾ Its wing geometry is quite equivalent to that in the 1st generation but its overall dimension and nose length are enlarged in order to install the ramjet engine and propellants required for supersonic missions. These enlargements will result in drag increase and deteriorate acceleration capability in transonic regime. Then some drag reduction in the transonic regime by the so-called area

rule is required. In addition, the proposed aerodynamic configuration with a large sweepback angle on the main wing, a high-wing geometry, and a large nose length will have the tendency of roll reversal in large AOA conditions caused by combination of large dihedral and adverse yaw effects and deterioration in directional stability. This paper describes such aerodynamic characteristics typical in the proposed 2nd-generation configuration for the supersonic flight experiment vehicle, on the basis of intensive wind-tunnel tests. In addition, flight capability predictions will be discussed on the basis of three- and six-degrees-of freedom flight trajectory calculations.

Section 2 describes the proposed aerodynamic configuration for the 2nd-generation vehicle design in comparison with the 1st-generation. Section 3 discusses the longitudinal, lateral, and control surface aerodynamics as well as roll reversal characteristics, on the basis of wind-tunnel tests. Section 4 overviews flight capability predictions. Section 5 describes some treatment for transonic drag reduction by the area rule. Then Section 6 is conclusions.

2. Proposed Aerodynamic Configurations

2.1. The first generation configuration

The first generation configuration called M2006prototype is illustrated in Fig.1. It has twin engines connected to the fuselage on its both sides. A diamond wing section of 6% thickness is adopted for reduction of wave drag during supersonic flights. Its main wing has a cranked-arrow planform for stable aerodynamic characteristics. A high-wing configuration with a dihedral of 1.0 degree is also adopted in order to attain sufficient roll stability. Its lateral control capability is enhanced by adopting all-pivoting elevons. Moreover, a pair of inboard flaps is installed for takeoff and landing.

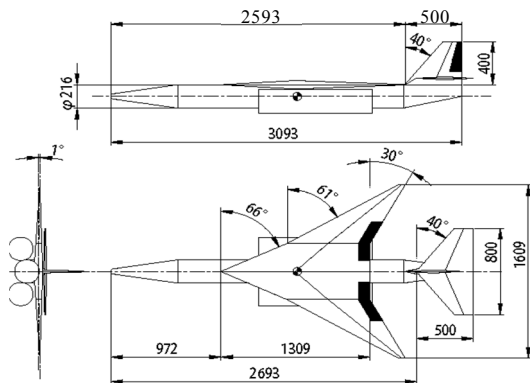


Fig. 1. The configuration M2006prototype for the first generation vehicle design.

2.2. The second generation configuration

A revised aerodynamic configuration M2011 with a single Air Turbo Ramjet Gas-generator-cycle (ATR-GG) engine is designed as shown in Fig. 2 and Table 1. Its wing and tail geometries are equivalent to those in the 1st

generation; most of the aerodynamic data for the 1st generation configuration can be applied to the 2nd generation. Its wingspan and fuselage diameter are enlarged by a factor of 1.5 so as to install an ATR-GG engine with a diameter of 230mm and to retain the ratio of wingspan to fuselage diameter. Three types of fuselage length, 5.8m, 6.8m, and 7.8m, are considered for various quantities of propellants loaded.

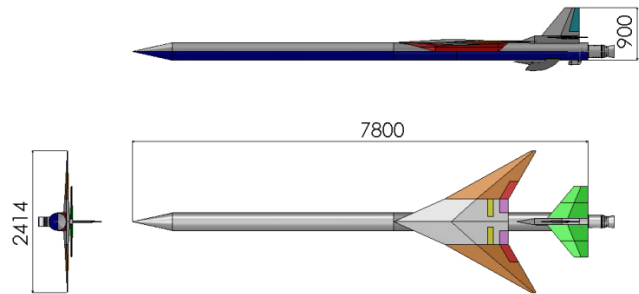


Fig. 2. The proposed revision configuration M2011 for the second generation vehicle design.

Table 1. Dimensions of the configurations M2006prototype and M2011.

	M2006-prototype	M2011
Wing Span [mm]	1609.0	2413.5
Wing Area [mm ²]	954856.8	2148427.8
Fuselage Diameter [mm]	200	300
Overall Length [mm]	3192	Nose A: 5800 Propellants 80kg
		Nose B: 6800 Propellants 105kg
		Nose C: 7800 Propellants 130kg

3. Aerodynamic Characterization

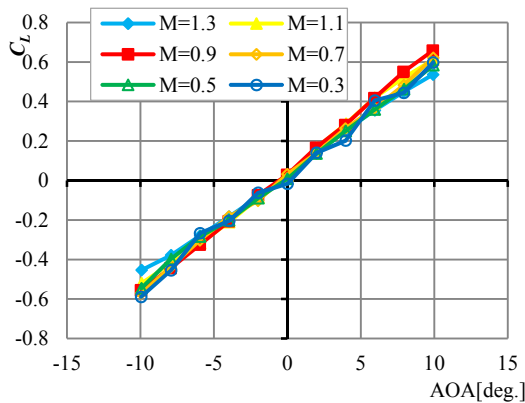
Generally, the cranked-arrow wing has good aerodynamic characteristics over a wide range of flight Mach number and angle of attack, because of its stable vortex system in the subsonic regime and its large sweepback angle suitable for the transonic/supersonic regimes. Such aerodynamics have been investigated in detail for wing-fuselage configurations without tails by Rinoie, Kwak, et al.⁴⁻⁸⁾ But those for overall configuration of practical vehicles with tails and control surfaces have not yet been clarified sufficiently. Thus the aerodynamic stability and controllability for the proposed overall configuration with tails and control surfaces are analyzed intensively in this development study.

3.1. Longitudinal aerodynamics

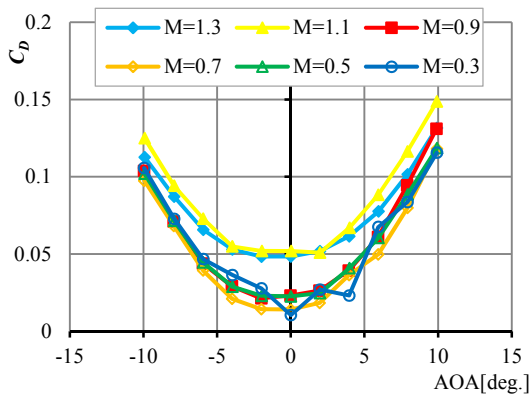
The transonic wind tunnel in the Comprehensive High-speed Flow Test Facility at the Institute of Space and Astronautical Science (ISAS) of the Japan Aerospace Exploration Agency (JAXA) and a Goettingen-type

subsonic wind-tunnel at Osaka Prefecture University are used for the present aerodynamic characterization. The transonic wind tunnel generates airflows of Mach 0.3 through 1.3. The results are shown in Figs. 3 and 4, and are summarized as follows:

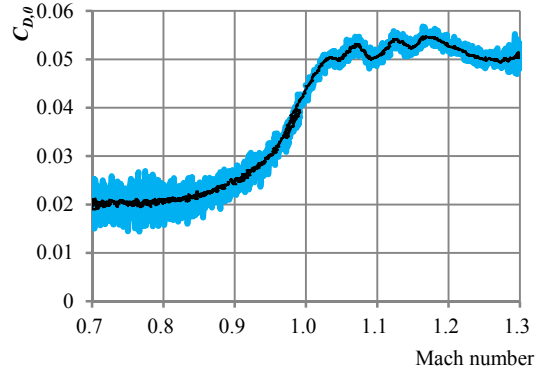
- ✓ The lift coefficient curves show quite a good linearity with a slope of 0.058/deg. for the subsonic, and 0.065/deg. for the transonic regime, where the elevators are fixed.
- ✓ The so-called sound barrier, i.e. the drag peak at the transonic regime, is small owing to the large sweepback angle of the main wing.
- ✓ According to the subsonic wind tunnel tests shown in Fig. 4, the linearity of the lift coefficient is found to be good for a wide range of AOA from -20 to +20 deg. It is probably owing to the stability of the vortex system over the present cranked-arrow wing with a large inboard sweepback angle of 66deg⁴).



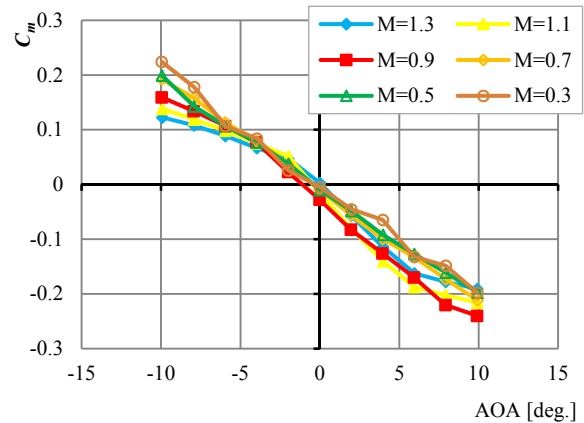
(a) Lift coefficient.



(b) Drag coefficient.



(c) Mach number dependence of the zero-lift drag coefficient.



(d) Pitching moment coefficient around the aerodynamic center of the main wing.

Fig. 3. Longitudinal aerodynamics for the 2nd generation configuration M2011 measured with the transonic wind-tunnel at JAXA/ISAS.

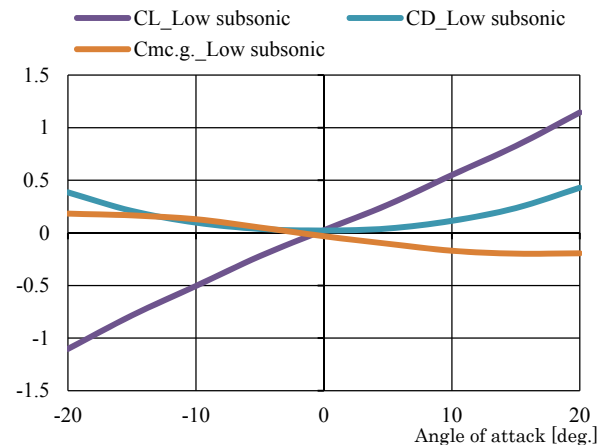


Fig. 4. Longitudinal aerodynamics for the 2nd generation configuration M2011 measured with the subsonic wind-tunnel at Osaka Prefecture University.

3.2. Influence of the nose and intake lengths of the configuration 2011 on longitudinal aerodynamics

Lift, drag, and pitching moment coefficients are measured for several sets of nose and intake lengths in the configuration M2011 and are illustrated in Fig. 5. Their influence on the longitudinal aerodynamics is found to be small.

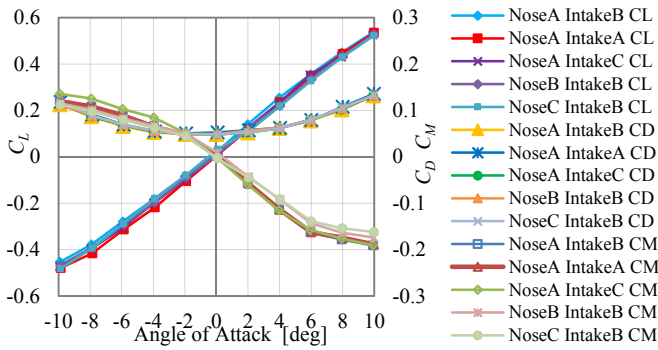
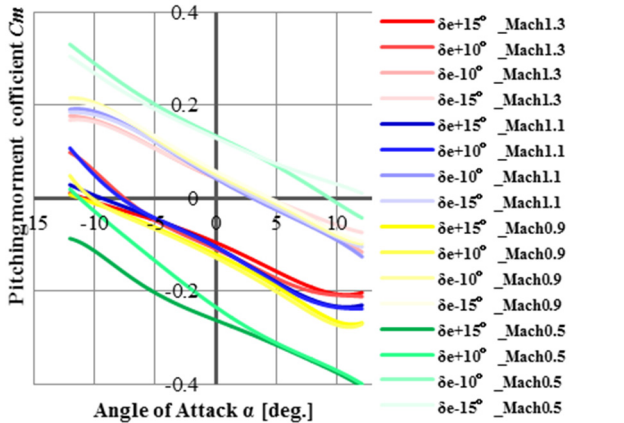


Fig. 5. Lift, drag, and pitching moment coefficients at Mach 1.3 for several sets of nose and intake lengths in the 2nd-generation configuration M2011.

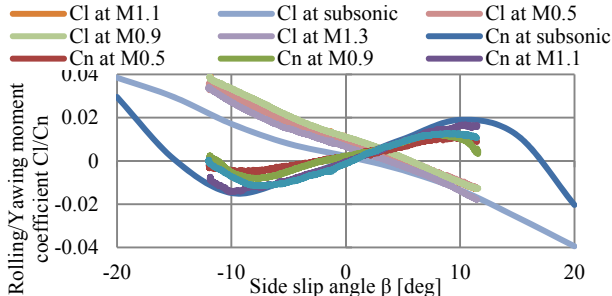
3.3. Trim capability, stability, and controllability for attitude motion

The measured variation of the pitching, rolling, and yawing moment coefficients of the 2nd-generation configurations M2011 with a nose C with and without control surface deflections were quite appropriate at small values of angles of attack and sideslip as shown in Fig. 6 for all Mach numbers ranging from 0.1 to 1.3.

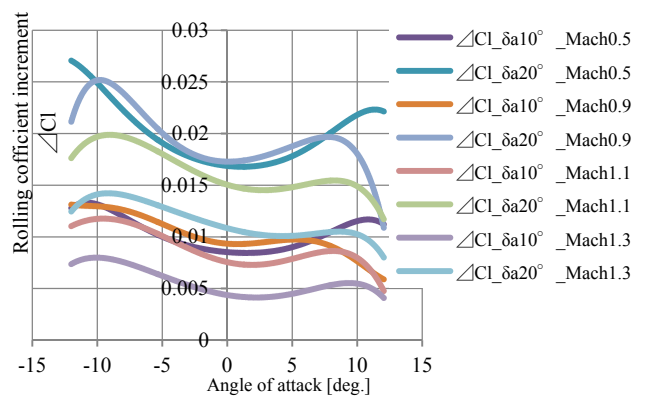
On the other hand, the directional stability deteriorates severely for values of angles of attack and sideslip larger than 10 degrees as shown in Fig. 6 (f). This is mainly caused by the large nose length of the configuration M2011 with a nose C and will be compensated with rudder deflections for angles of attack and sideslip up to 12 degrees, according to the rudder effectiveness shown in Fig. 6 (e). In addition, Fig. 6 (g) shows that some adverse yaw effects take place owing to elevon deflections.



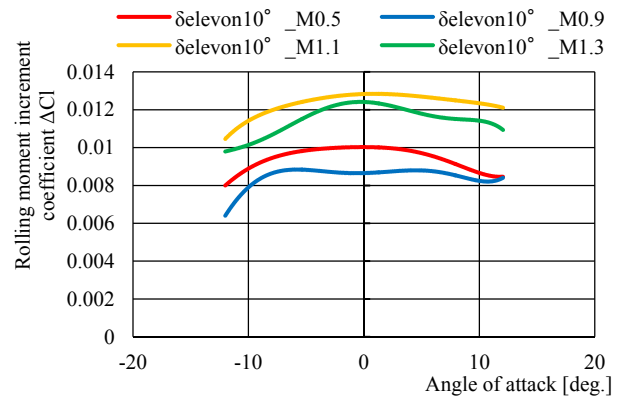
(a) Pitching moment coefficient around the aerodynamic center (25%MAC) for several elevator deflections.



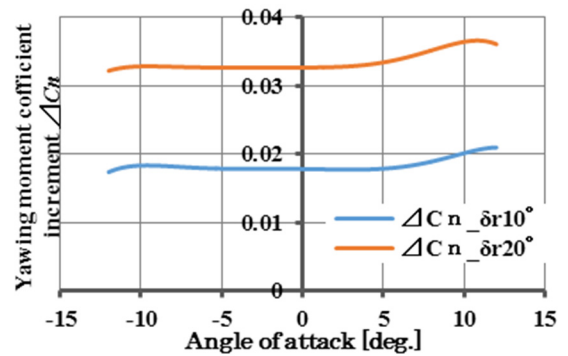
(b) Rolling and yawing moment coefficients at zero angle of attack vs. sideslip angle.



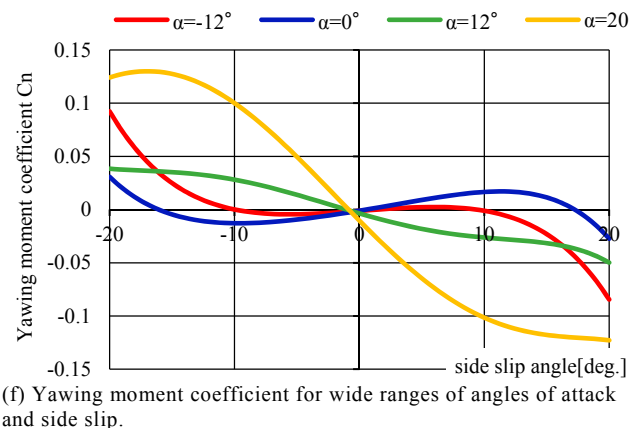
(c) Rolling moment coefficient caused by aileron deflections.



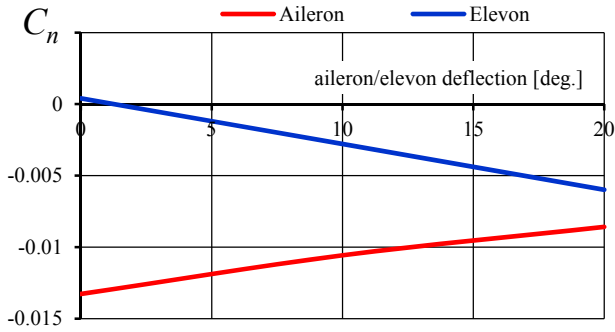
(d) Rolling moment coefficient caused by elevon deflections.



(e) Yawing moment caused by rudder deflections.



(f) Yawing moment coefficient for wide ranges of angles of attack and side slip.



(g) Yawing moment caused by aileron and elevon deflections at zero angle of attack.

Fig. 6. Aerodynamic moment coefficients for the 2nd-generation configuration M2011 with a nose C with and without control surface deflections measured by wind tunnel tests.

3.4. Lateral control departure characteristics

The roll control capability by aileron deflection would deteriorate at high angles of attack typically on taking-off and landing, owing to dihedral and adverse yaw effects and deterioration in directional stability. Such characteristics are assessed by the so-called aileron alone departure parameter (AADP):⁹⁾

$$\text{AADP} = C_{n,\beta} - \frac{C_{n,\delta_a}}{C_{l,\delta_a}} C_{l,\beta} \quad (1)$$

The negative values of AADP indicate negative aileron effectiveness i.e. roll reversal. Here in ordinal winged vehicle configurations, C_{l,δ_a} is positive due to effectiveness of ailerons itself and $C_{l,\beta}$ is negative due to rolling stability, i.e. dihedral effects. Then the primary causes of the negative values of AADP are negative values of C_{n,δ_a} due to adverse yaw effects and small or negative values of $C_{n,\beta}$ due to deterioration in directional stability, in combination with small values of C_{l,δ_a} and large values of $C_{l,\beta}$.

Such characteristics of roll reversal can be prevented by a coordinated rudder deflection. In this occasion, the rolling capability is assessed with the lateral control departure parameter (LCDP):

$$\text{LCDP} = C_{n,\beta} - \frac{C_{n,\delta_a} + kC_{n,\delta_r}}{C_{l,\delta_a} + kC_{l,\delta_r}} C_{l,\beta} \quad (2)$$

where $k = \delta_r/\delta_a$ is the rudder gain. In addition, the 2nd-generation configuration M2011 has a pair of elevons which will be deflected in a coordinated manner with ailerons. Thus a modified LCDP including elevon deflections is applied:

$$\text{LCDP} = C_{n,\beta} - \frac{C_{n,\delta_a} + kC_{n,\delta_r} + k_e C_{n,\delta_e}}{C_{l,\delta_a} + kC_{l,\delta_r} + k_e C_{l,\delta_e}} C_{l,\beta} \quad (3)$$

where $k_e = \delta_e/\delta_a$ is the elevon gain.

Fig. 7 shows the evaluated AADP/LCDP for the configuration M2011 with a nose-C on the basis of

subsonic wind-tunnel tests. The green curve for the AADP shows negative roll capability at angles of attack above 7 degrees which take place easily on taking-off and landing. This roll reversal tendency is prevented at angles of attack up to 12 degrees by a coordinated rudder deflection with a rudder gain of 0.5 as shown by the blue curve for the LCDP. Additional coordinated elevon deflection makes the roll capability worse as shown by the red curve. It is because of the adverse yaw effects of the elevon deflection indicated in Fig.6 (e). Thus a supplementary utilization of elevons for roll control is not appropriate for the proposed 2nd-generation configuration.

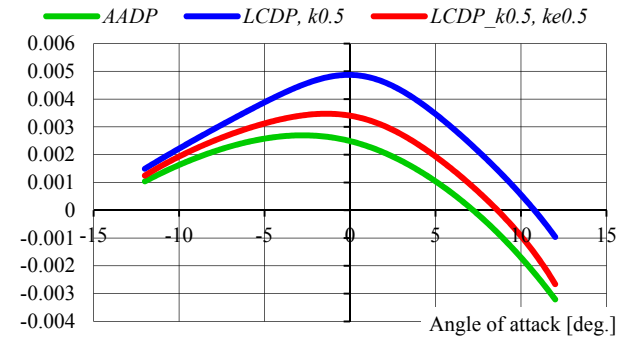


Fig. 7. Evaluated AADP/LCDP for the 2nd-generation configuration M2011 with a nose-C on the basis of wind-tunnel tests.

4. Flight Capability Predictions

The thrust margin, i.e. thrust minus zero-lift drag, was evaluated for the proposed 2nd-generation configuration M2011 with an ATR-GG engine, on the basis of the wind-tunnel tests and the engine design analysis. The results are illustrated in Fig. 8 with respect to flight Mach number and altitude. A narrow corridor is shown in the transonic region and a saddle point exists at about Mach 1.3 and 11km altitude. The vehicle must fly through this saddle point and the corridor in order to reach the supersonic regime.

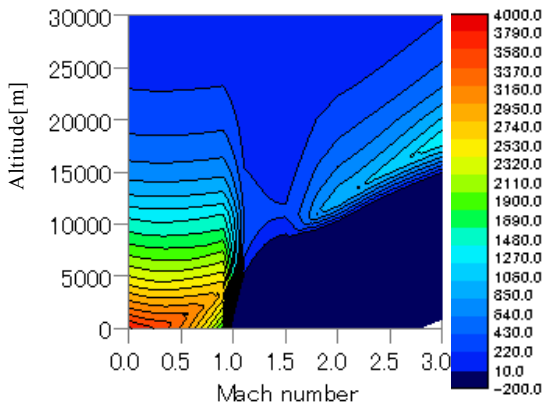
Flight trajectory analysis of three degrees of freedom, i.e. point mass analysis was carried out for several conditions on engine rotation, loaded propellant mass, prospective reduction in drag and structural weight. One of the results is shown in Fig. 9, where an engine rotation of 105% and a loaded propellant of 130kg (correspondent to the Nose-C and a fuselage length of 7.8m) were assumed. This result indicates that some enhancement in thrust and/or reduction in drag are required for a flight capability to reach Mach 2.0.

In addition, a six-degree-of-freedom flight simulation system was constructed on the basis of the following equations of attitude motion:¹⁰⁾

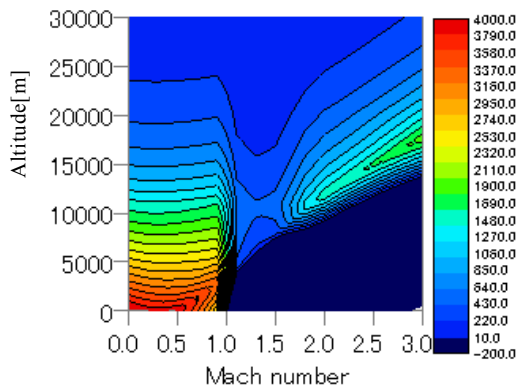
$$\begin{bmatrix} \dot{L} \\ \dot{M} \\ \dot{N} \end{bmatrix} = I\dot{\vec{\Omega}}_b + \vec{\Omega}_b \times (I\vec{\Omega}_b) \quad (3)$$

where $\vec{M}_b = [L, M, N]^T$ is the aerodynamic moments with

respect to the body-fixed coordinates, I is the moment-of-inertia matrix, and $\vec{\Omega}_b$ is the angular velocity vector with respect to the body-fixed coordinates. An analysis code is composed using the MATLAB/ Simulink¹¹⁾ and flights of the 2nd-generation vehicle with the configuration M2011 Nose-A were solved. Their results illustrated partly in Fig. 10 show that the vehicle will take off from the Taiki Flight Experiment Airfield after running 400 meters for about 10 seconds on the runway. It makes a round flight with a maximum altitude of 11km and a maximum Mach number of 1.15. Its downrange is 45km and the flight duration is 550 seconds.

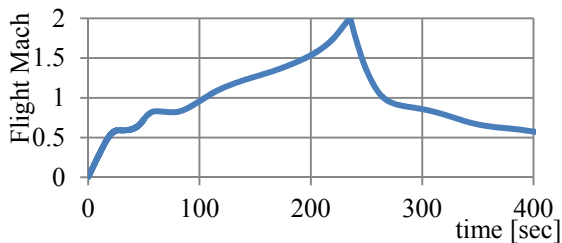


(a) Nominal rotation of the engine.

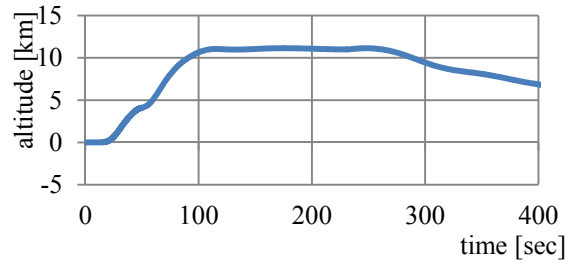


(b) 105% rotation of the engine.

Fig. 8. Evaluated thrust margin [N] for the 2nd- generation vehicle with an ATR-GG engine.

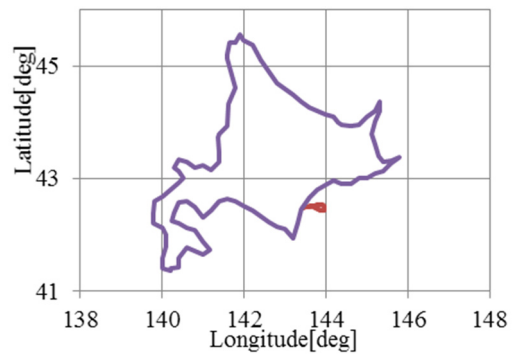


(a) History of the flight Mach number.

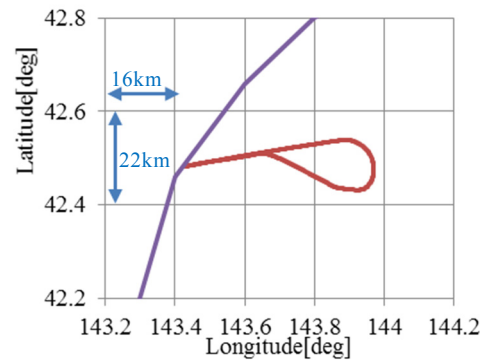


(b) History of the flight altitude.

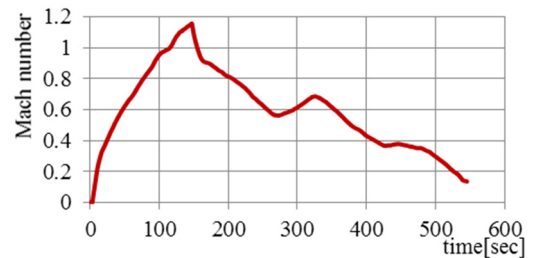
Fig. 9. Results of the three-degree-of-freedom flight analysis for the 2nd-generation vehicle with a nose C, i.e. loaded propellant of 130kg. An engine rotation of 105% are also assumed.



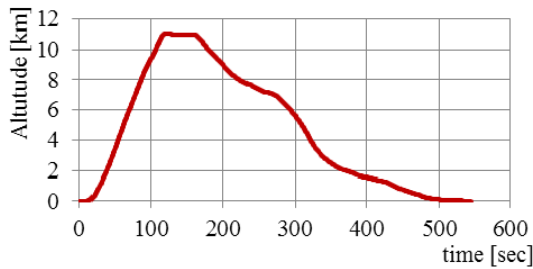
(a) Flight trajectory.



(b) Zoomed flight trajectory.



(c) History of the flight Mach number.



(d) History of the flight altitude.

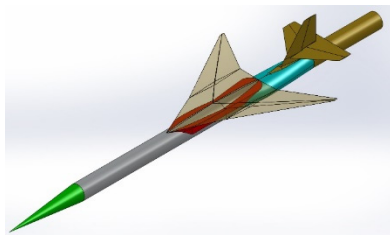
Fig. 10. Results of the six-degree-of-freedom flight analysis for the 2nd-generation vehicle with a nose A.

5. Drag Reduction in Transonic Regime

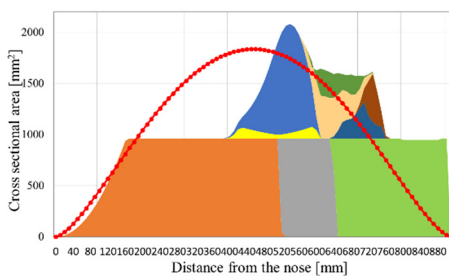
As indicated in the thrust margin and flight trajectory analyses, some reduction in transonic drag is required for a sufficient flight capability to reach the supersonic regime. Such reduction can be attained by modification of the aerodynamic configuration on the basis of the so-called area-rule, so as to make the cross sectional area distribution close to the Sears-Haack curve. Fig. 11 shows a trial modification composed of the following elements:

1. sharpening the nose : AR-Nose C
2. moving the wings and tails forward
3. adding a pair of bulges on the fuselage between the main wing and the tails: Bulge A and Bulge B

The results of a wind-tunnel test for several sets of above modification elements are illustrated in Fig. 12. The sharpened AR-Nose C attains a drag reduction for a wide range of Mach number from 0.9 to 1.2, whereas the wing/tails forward movement and the bulges are effective only at Mach 1.1 to 1.2. As a results, 5 to 20 % drag reduction in the transonic regime can be attained by these modifications. More detailed tests and analysis are to be carried out.



(a) Overall appearance.



(d) The cross-sectional area distribution at Mach 1.1.

Fig. 11. The configuration M2011 with a nose C modified by the area rule.

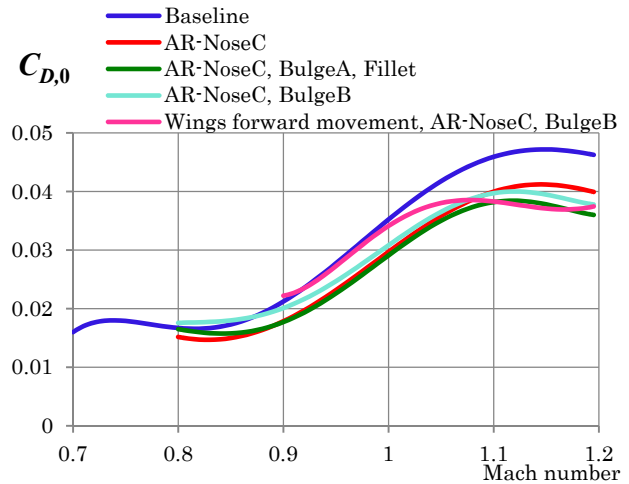


Fig. 12. Results of preliminary wind-tunnel tests on the reduction in zero lift drag by the area rule.

6. Conclusions

With the aims of creating and validating innovative fundamental technologies for high-speed atmospheric flights, a small scale supersonic flight experiment vehicle was designed as a flying test bed. An aerodynamic configuration was proposed for the 2nd-generation vehicle with a cranked-arrow main wing and a single Air Turbo Ramjet Gas-generator-cycle (ATR-GG) engine. Its longitudinal, lateral, and control surface aerodynamics were characterized through intensive wind-tunnel tests. They were found to be quite moderate except that the directional stability deteriorates severely at large angles of attack and side slip, and that the elevon deflections for roll control cause adverse yaw. These aerodynamic anomalies will result in a tendency of roll reversal at large angles of attack. It can be prevented to some extent by coordinated rudder deflections. In addition, necessity of transonic drag reduction was clarified through thrust margin and flight capability analyses. Probability of 5 to 20 % drag reduction in the transonic regime (Mach 0.8 to 1.2) was demonstrated by configuration modification on the basis of the area rule at Mach 1.1.

Acknowledgments

The authors would like to express cordial gratitude to JAXA/ISAS for having given opportunities of wind tunnel tests at its Comprehensive High-speed Flow Test Facility.

References

- 1) Minato, R., Kato, D., Higashino, K. and Tanatsugu, N.: Development Study on Counter Rotating Fan Jet Engine for Supersonic Flight, ISABE 2011-1233, Goteborg, Sweden, 2011.
- 2) Mizobata, K., Minato, R., Higuchi, K., Ueba, M., Takagi, S., Nakata, D., Higashino, K. and Tanatsugu, N.: Development of a Small-scale Supersonic Flight Experiment Vehicle as a Flying

- Test Bed for Future Space Transportation Research, *Transaction of JSASS, Aerospace Technology Japan*, **12**, No.ists29 (2014), pp.Po_3_1-Po_3_10.
- 3) Minato, R., Higashino, K. and Tanatsugu, N.: Design and Performance Analysis of Bio-Ethanol Fueled GGcycle Air Turbo Ramjet Engine, AIAA Aerospace Science Meeting 2012, Nashville, Tennessee, USA, 2012.
 - 4) Kwak, D., Rinoie, K. and Kato, H.: Longitudinal Aerodynamics at High Alpha on Several Planforms of Cranked Arrow Wing Configuration, 2010 Asia-Pacific International Symposium on Aerospace Technology, Xian, China, September 13-15, 2010.
 - 5) Kwak, D., Noguchi, M., Shirotake, M. and Rinoie, K.: Rolling Moment Characteristics of Supersonic Transport Configuration at High-Incidence Angles, *Journal of Aircraft*, **43** (2006), No. 4, pp.1112-1119.
 - 6) Kwak, D., Hirai, K., Rinoie, K. and Kato, H.: Rolling Moment Characteristics at High Alpha on Several Planforms of Cranked Arrow Wing Configuration, 27th AIAA Applied Aerodynamics Conference, 22-24 June 2009, San Antonio, Texas, USA.
 - 7) Kwak, D., Shirotake, M. and Rinoie, K.: Vortex Behaviors over a Cranked Arrow Wing Configuration at High Angles of Attack, 24th International Congress of the Aeronautical Sciences, 29 August - 3 September 2004, Yokohama, Japan.
 - 8) Hirai, K., Kwak, D. and Rinoie, K.: Vortex Behaviors of Cranked Arrow Wing Configurations with Different Wing Planforms, 26th International Congress of the Aeronautical Sciences, 14 - 19 September 2008, Anchorage, Alaska, USA.
 - 9) Pamadi, B. N.: *Performance, Stability, Dynamics, and Control of Airplanes*, AIAA, 2004.
 - 10) McFarland, Richard E.: A Standard Kinematic Model for Flight Simulation at NASA-Ames, NASA CR-2497, 1975.
 - 11) Jackson, E. B., and Cruz, C. L.: Preliminary Subsonic Aerodynamic Model for Simulation Studies of the HL-20 Lifting Body, NASA TM4302, 1992.